2024

Modelling And Simulation Of A Carnot Battery Coupled To Seasonal Underground Stratified Thermal Energy Storage For Heating, Cooling And Electricity Generation.

Aitor Cendoya
University of Liège, acendoya@uliege.be

Frederic Ransy
University of Liège, frederic.ransy@uliege.be

Vincent Lemort
University of Liège, vincent.lemort@uliege.be

Andres Hernandez
University of Liège, jahernandez@uliege.be

Pierre Dewallef
University of Liège, P.Dewallef@uliege.be

See next page for additional authors

Authors

Aitor Cendoya, Frederic Ransy, Vincent Lemort, Andres Hernandez, Pierre Dewallef, Pierre-Henri Gresse, and Jacques Windeshausen

Modelling and Simulation of a Carnot Battery Coupled to Seasonal Underground Stratified Thermal Energy Storage for Heating, Cooling and Electricity Generation

Aitor CENDOYA[1]*, Frederic RANSY[1,2], Vincent LEMORT[1], Andres HERNANDEZ[1], Pierre DEWALLEF[1], Pierre-Henri GRESSE[3], Jacques WINDESHAUSEN[2]

[1]Thermodynamics Laboratory, Faculty of Applied Sciences,
University of Liège, Liège, Belgium

[2]Wingest Energy,
Bastogne, Belgium

[3] Flexide Energy,
Liège, Belgium

*corresponding author (acendoya@uliege.be)

ABSTRACT

Nowadays, most countries are striving to transition their energy matrices towards renewable sources. To achieve this goal, energy storage systems play a crucial role in compensating for the inherent intermittency of renewable sources. Buildings are among the largest consumers of primary energy, due to their heating demands. Consequently, integrating renewable energies into buildings is essential. This paper presents a pioneering approach that integrates renewable energy sources with a multi-energy system. This system powers a Heat Pump (HP) responsible for heating an abandoned mine flooded with water, producing electricity via a Carnot Battery (CB), and distributing heating and cooling through a district heating network (DHN).This study is conducted in a real case of an abandoned slate mine in Martelange, Belgium, where three different size caverns are employed to store energy: 800, 6840, and 80000 m^3 for hot (90°C), medium (50°C), and cold (5°C) water temperature, respectively. The system combines photovoltaic panels, an electrical battery, heat pumps, electrical resistance, and an Organic Rankine Cycle. This study highlights the potential of reusing abandoned mines as energy storage systems, which can benefit adjacent communities by integrating diverse energy demands within a single system. This generates new perspectives for investors and residents, enabling the possibility of connecting the system to the grid for energy arbitrage and balancing services.

1. INTRODUCTION

The building sector is one of the largest contributors of carbon dioxide (CO_2) worldwide (Cabeza et al., 2022). Therefore, it is imperative to explore solutions to mitigate its greenhouse gas emissions, which is in line with the latest protocols and agreements aimed at limiting the increase in emissions and addressing the current climate crisis. The transition of the energy matrix and heat sources towards Renewable Energy Sources (RES) is crucial. Nevertheless, increasing energy production brings together an additional challenge, as it requires a larger storage capacity in the electrical grid due to its inherent intermittency, in order to decouple energy demand from electricity production (Olympios et al., 2020). Among the different storage systems available, Thermal Energy Storage (TES) is highlighted as a large-scale solution, allowing integration with various infrastructures such as District Heating Networks (DHN). In this context, Seasonal TES (STES) have the advantage of storing energy generated during periods of non-excess usage and high production, to then deliver it when demand is higher. These storage systems offer the benefit of extended lifespan and low investment costs (Luo et al., 2015). It is also possible to implement an Organic Rankine Cycle (ORC) as a heat-to-power conversion system (Dumont et al., 2020). The flexibility of these systems allows the production of heat through RES and the generation of electricity through an ORC. These systems are known as Carnot Batteries (CB) or Thermally Integrated-Pumped Thermal Energy Storage (TI-PTES).

ORC power systems have been extensively researched due to their remarkable potential to generate electricity from low-temperature heat sources (Poletto et al., 2024), with the additional benefit that integrating these technologies with multi-energy systems could lead to a significant increase in the overall performance. The dynamics of the ORC have

been the subject of numerous studies, such as the one conducted by (Desideri, 2016), who identified that the system dynamics and the heat inertia time are due mainly to heat exchangers. One aspect that has not yet been fully explored is the feasibility of these systems to provide ancillary services to the electrical grid, allowing for the production and absorption of electricity to maintain its regulation. Therefore, this paper presents a case study of a CB concept connected to a flooded abandoned slate mine in southern Belgium, able to store and produce heat, cold and electricity. Nowadays, the connections between the chambers and the components are being carried out. The idea is to create different Seasonal Underground Stratified TES (SUSTES) destined for different purposes to store energy at a High Temperature (HT, 90°C), Medium Temperature (MT, 45°C) and Low Temperature (LT, 5°C). The objective of this work is to propose a novel multi-energy integration for a residential complex of 50 apartments, implementing and supporting the uses of RES for supplying heating and cooling to nearby stakeholders. To achieve this, Photovoltaics Panels (PV) are coupled with an electrical battery for being self-consumed by the main HP which stores heat in the MT reservoir. Additionally, the CB is employed for charging and discharging the HT reservoir, seeking to dispatch electricity to the Belgian grid while providing ancillary or balancing services to the grid.

2. METHODOLOGY

2.1 Electricity Overview
The electricity market is composed of a series of companies that seek to sell electricity, supply the electricity demand of consumers and maintain a stable grid frequency and voltage. Distribution System Operators (DSO) and Transmission System Operators (TSO) have different contracts and trading platforms for this service. The Belgian Electricity Exchange (BELPEX) is a wholesale trading platform where producers and consumers trade electricity. This platform offers two different markets such as the daily market (DAM) where participants trade electricity bids and know the price and volume the day before delivery after the market clearing process. The second market corresponds to the intra-day market (IDM), which allows trading and purchasing energy blocks by hourly periods, up to one hour before delivery. On the other hand, balancing or ancillary services are part of the regulation market, to keep the frequency and voltage of the grid constant. The TSO balancing market consists of three service classifications: Frequency Containment Reserve (FCR), automatic Frequency Restoration Reserve (aFRR) and manual Frequency Restoration Reserve (mFRR). The difference within the system is mostly the response time which corresponds to within seconds, 7.5 min and 15 min, respectively and the maximum duration of an activation.
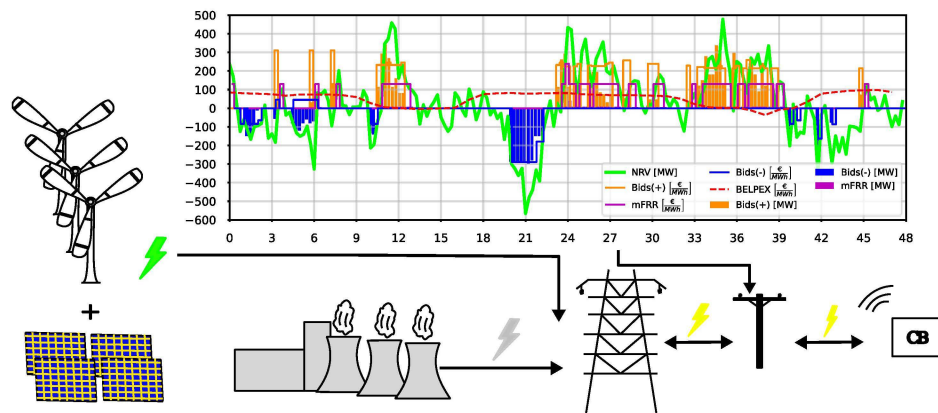

Figure 1: Diagram of electricity distribution in the study system with a two-day electricity market forecast.

The main objective is to adjust the grid to the required frequency and voltage, which seeks to balance the actual energy production from the generators to the one programmed. To achieve this, two regulation signals can be received, upward (+) or downward (-), the first corresponds to a power deficit in the grid and the second to when there is excess power in the grid. Figure 1 presents the electricity flow of the power unit in the study system, which corresponds to a CB participating in the DAM and balance-of-grid services, specifically as a tertiary service (mFRR). The Figure presents the Net Regulation Volume (NRV), i.e. the volume of control energy to maintain the balance. This value, subtracted from the Area Control Error (difference between the programmed values and the energy measured in the network) allows obtaining the grid imbalance (SI). For the mFRR, the energy revenues correspond to the amount of energy supplied by the upward or downward bids and their respective price. The amount of energy supply is the request volume by the TSO which depends on the proposed bid price (€/MWh) and its position in the mFRR merit

order. In addition, there is a revenue for holding the system available for service, which is not considered in this paper, only the energy consumed/produced and the respective price of each offer are considered in the calculation of the revenue. The energy offers, volumes and prices are extracted from historical data available on Elia's website, and correspond to the price and energy of the year 2023, with a time step of 15 minutes. These data are considered throughout the 4 years of the system simulation assuming a similar behaviour.

The operating strategy of the system is to always prioritise mFRR, even if the price of BELPEX is more profitable than mFRR. However, if there is no demand for it, the system will privilege the DAM, extracting electricity to the grid, when the price is below 0 €/MWh, and injecting electricity when the price is higher than 100 €/MWh.

2.2 Study site
The study site is an abandoned slate mine located in the south of Belgium, in the town of Martelange. This place had mining activities until 1990 when it was closed. Today the mine has no activities and over the years the water permeated between the rocks and filled the chambers, reaching a value of 500000 m^3, distributed in 9 chambers. These interconnected chambers have a maximum depth of 180 m, decreasing from east to west. Figure 2 presents the actual study site with the 3-D representation of the chambers. The main objective is to assess the feasibility of using the underground cavern for energy storage purposes. In this study 3 caverns are used as energy storage: 800 m^3 at HT (90-70°C), 6840 m^3 at MT (50-40°C) and 80000 m^3 at LT (10-5°C). These values are the existing volumes of caverns available in the abandoned mine. The different temperatures are selected to be used by the ORC, to cover the heating demand by the DHN, and the last one for the cold storage (which is still looking for stakeholders).
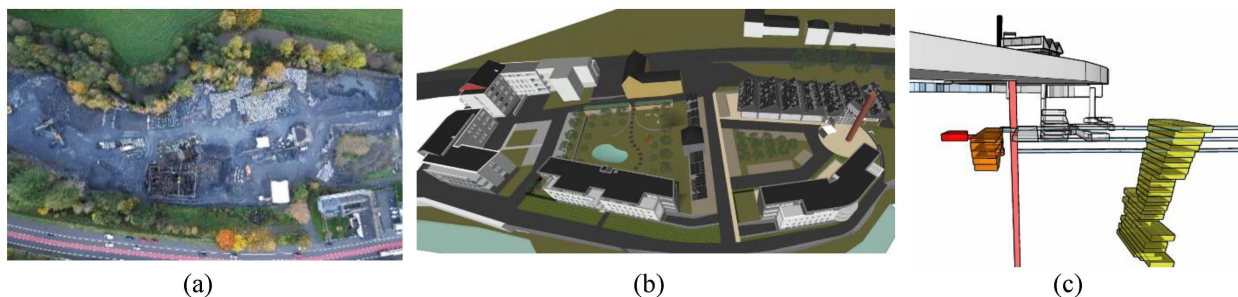

| (a) | (b) | (c) |

Figure 2: Abandoned mine a) actual condition, b) future condition and c) the 3 assessed chambers for the study site.

The climatic conditions at the study site correspond to a typical year extracted from EnergyPlus (Crawley et al., 2001). These conditions start from 1 January to 31 December at 1-hour intervals. The average dry bulb temperature corresponds to 7.4 °C, the average global horizontal radiation is 113.6 Wh/m^2, and the average relative humidity is 82.9%. The mean relative ambient pressure does not show considerable changes, reaching a value of 0.94 atm, respectively. This meteorological file is considered for the 4-year simulation.

2.3 Models
This section describes the dynamic model of the components used for this study that are implemented in Dymola and corresponds to the buildings, radiant slab, buffer tank, underground reservoirs, DHN, HPs, CB (which considers Electrical Resistance (ER), HP and an ORC), PV and an Electric Battery.

2.3.1 Buildings: The assessed residential complex consists of 50 apartments, distributed in 5 buildings. They share identical infrastructure, construction materials and distribution within the floors. Each apartment is discretised into thermal zones, which are connected by the block available in the IDEAS library. This model considers the heat transfer between the different layers of materials that integrate the different walls (internal, opaque and windows), besides it considers the different types of radiation (internal longwave and shortwave radiation (window)) within each zone. Insights of this are presented by Jorissen et al. (2018). The occupant's comfort is assessed according to Fanger's theory, which considers an office work activity for the occupant's schedule. The total area of the building complex corresponds to 8906 m^2, where each apartment has a maximum height of 3 m.

2.3.2 Radiant Slab: The model used corresponds to the block Radiant slab from the IDEAS library. This model assumes that the radiant slab is located at half of the floor depth. The parameters of the radiant slab are based on EN 15377-1. It considers *n* number of discretizations, which allows the computation of the partial heat accumulation and

then integrates the values to calculate the overall result, the equivalent thermal conductance of the circuits and the thermal resistance are used for this purpose. Each apartment circuit has a three-way valve that facilitates the connection between them and the buffer tank, aiming to regulate the temperature of the circuit to 35°C, through a PI control. The pump of the circuit aims to regulate a set-point temperature within the zones of 18 ± 0.25°C from 24 p.m. and 7 a.m., and 20 ± 0.25°C from 7 a.m. to 24 p.m. For the cooling mode, the underground water of the LT reservoir is directly sent to the radiant loop, where the three-way valve sets a temperature of 12°C. The set-point temperature in the zones corresponds to 27 ± 0.25 °C.

2.3.3 Buffer Tank: Each apartment is equipped with its own buffer tank, which distributes hot water for both, space heating (SH) and Domestic Hot Water (DHW). The tank model corresponds to a modification of the StrafidiedEnhancedInternalHex block available in the IDEAS library, allowing the connection of 3 heat exchangers (HE). The first one corresponds to the exchange with a HP to boost the water temperature at 55°C for the DHW, the second transfers heat to the radiant slab (SH) circuit and the third one extracts heat from the DHN. In addition, 1.5 kW of ER is used as a back-up system. The total volume of the tank corresponds to 300 L, where every day 200 L are withdrawn for DHW, which are replaced with tap water at 12°C. The control seeks to maintain stratification inside the tank through the use of 3 ON-OFF set points. The first one aims to always keep temperatures between 50-55°C at the top of the tank, therefore the HP will turn on or off, the second one corresponds to the ER which aims to maintain 45°C in the middle of the tank and the last one which aims to maintain a bottom temperature between 40-45°C by taking heat from the DHN.

2.3.4 Underground Reservoirs: The thermodynamic properties of the underground reservoirs correspond to the slate properties with a thermal conductivity (λ) of 2.57 W m^{-1}K^{-1}, a density (ρ) of 2750 kg m^{-3} and a specific heat (c_p) of 837 J kg^{-1}K^{-1}. The assumed initial soil temperature corresponds to 10°C, based on the reported average soil temperature (Grabenweger et al., 2021). The model used corresponds to the n mixing volumes connected to the resistances and capacitances which represent the thermal inertia of the slate. The mixing volumes combine all water flows with uniform pressure in the volume (Wetter & Van Treeck, 2017). In addition, the model considers the transient terms in the mass and energy balance in the volumes. For the HT reservoir, ERs are used to reach 90°C, because it is more complex to reach these high temperatures with a HP. The heat extraction from the reservoir is driven by the ORC and the back-up HP (bk HP) is only used for the 1st and 2nd years (due to the fact that the temperature is lower than 60°C). The charging phase of the MT-SUSTES is performed by the main HP and the bk HP for the 3rd and 4th years. The discharge is conducted by the DHN, which is in charge of distributing heat to the apartments.

2.3.5 District Heating Network: This component corresponds to the transmission system between the underground reservoirs and the end users in each apartment. The block used corresponds to the PlugFlow pipe model available in the library of the International Building Performance Simulation Association (IBPSA). This model considers a direct contact between the pipe insulation and the ground, which is considered to be equal to 10 °C without time variation. The pressure drop is associated with the mass flow rate by a quadratic relationship that has a constant value, called K. This constant depends on the equivalent length and the pressure drop at nominal conditions (Wetter & Van Treeck, 2017). The total distance of the model corresponds to 330 m with a potential height increase of 50 m.

2.3.6 Carnot battery: The CB is one of the crucial elements in this work as it is responsible for producing electricity and converting the electricity into heat to be stored. This battery is composed of an ORC, a HP, and ERs. The nominal power of the ORC corresponds to 48 kW$_e$ at 90°C in the evaporator and 10°C in the condenser, within an expander speed of 75 Hz, the working fluid of the ORC corresponds to R1233ZD. The ORC system employs a screw expander with a swept volume of 3 m^3 h^{-1}. On the other hand, the bk HP has a nominal heat output of 60 kW$_{th}$, this system operates with R410A. In addition, 800 kW of ERs are used in the HT reservoir to reach 90 °C when the mFFR is downward or the BELPEX price is below 0 € MWh^{-1}. The ORC is one of the key systems which requires the longest time to reach its nominal condition, so the start-up and shut-down times must be taken into account. For that, a transfer function which considers the stabilization time of the heat exchangers (HEs) is considered, whilst the expander time is neglected because its response is considerably lower than the HEs (Desideri, 2016). The transfer function is identified from experimental data obtained during the start-up of a small-scale ORC system (11 kW) fully described in (Desideri et al., 2016). The input-output data is normalized as the main interest is to define the time range the system takes to reach steady-state conditions. Thus, a second-order transfer function is identified using the prediction error minimization method described in (Ljung, 1999), for a sampling time of 1 second. The validation of the prediction is presented in Figure 3, the capabilities of the transfer function are assessed using two different sets of start-up data, providing a data fit above 82%, with an average fit of 86%. Notice that in this first phase, it is assumed that the

behaviour of the ORC studied is similar to the one described by Desideri et al. (2016), as both have the same volumetric machine, however, in further stages, this transfer function will be related to the residence time of the fluid inside the heat exchangers, to realise a general function.
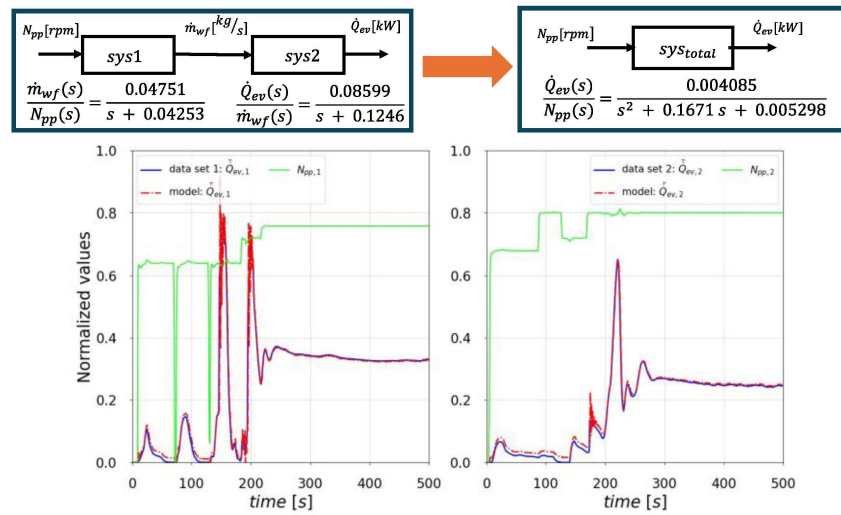
$$N_{pp}[rpm] \quad \boxed{sys1} \quad \dot{m}_{wf}[kg/s] \quad \boxed{sys2} \quad \dot{Q}_{ev}[kW]$$

$$\frac{\dot{m}_{wf}(s)}{N_{pp}(s)} = \frac{0.04751}{s + 0.04253} \qquad \frac{\dot{Q}_{ev}(s)}{\dot{m}_{wf}(s)} = \frac{0.08599}{s + 0.1246}$$

$$N_{pp}[rpm] \quad \boxed{sys_{total}} \quad \dot{Q}_{ev}[kW]$$

$$\frac{\dot{Q}_{ev}(s)}{N_{pp}(s)} = \frac{0.004085}{s^2 + 0.1671\,s + 0.005298}$$

Figure 3: Validation of the second-order transfer function identified based on experimental data.

The ORC model corresponds to a thermodynamic model that considers the real irreversibility that occurs in a system. Table 1 presents the parameters considered in the ORC simulation. This system uses a control strategy in the secondary fluid feed pumps to obtain a glide of 10 K in the evaporator and 5 K in the condenser.

Table 1. Organic Rankine Cycle parameters.

$\Delta T_{pp,ev}\ [K]$	$\Delta T_{pp,cd}\ [K]$	$\varepsilon_{s,exp}\ [-]$	$\varepsilon_{v,exp}\ [-]$	$\varepsilon_{s,pp}\ [-]$	$\Delta T_{sh}\ [K]$	$\Delta T_{sc}\ [K]$	$N_{exp}[Hz]$
5	5	0.61	0.95	0.7	5	3	75

2.3.7 Heat Pumps: The HPs correspond to the water-water type, where the selected block is extracted from the IDEAS library (Jorissen et al. (2018)). The system parameters are selected according to the manufacturer Viessmann, model Vitocal 300G BW301.A29. The model considers the epsilon-NTU methods and an empirical model for the compressor, according to Jin (2002). For the heat exchangers, the UA (model parameter) is related to the capacitive flow rate, which depends on the supply conditions. For the compressor, the theoretical consumption power is calculated, and the dynamic effect is represented by the compressor speed and the operation conditions. Two HPs are considered, the bk HP mentioned previously and the main one, which has a nominal heat power ($\dot{Q}_{cd}$) corresponding to 140 kW$_{th}$. The main HP self-consumes the electricity produced by the PV array through an electric battery. Therefore, while the SOC of the battery is between 99% and 10%, the HP operates at nominal capacity. When the SOC drops below 10%, it stops until the SOC reaches 50% again, to operate for at least 1.5 hours. For the first two years, the bk HP operates in the HT reservoir to reach 60°C, then during the 3rd and 4th years serves as a backup for the MT reservoir when the temperature drops below 40°C.

2.3.8 Photovoltaic panels: The area of the PV panels corresponds to 400 m^2 with an inclination angle of 30°, to optimize the conversion efficiency of the solar energy. The block used corresponds to the PVSystemGeneral available in the IDEAS library, which corresponds to the 5-parameter model of Duffie & Beckman (1991). This represents the system as a single-diode equivalent. The electricity produced is injected directly into the electric battery and when the SOC is higher than 99% the electricity is used in the study site through the auxiliary components.

2.3.9 Electric battery: This component stores the PV electricity for self-consumption through the main HP. The model corresponds to a battery with stackable ionic cells, which is modelled according to the Modelica Standard Library. The battery capacity corresponds to 550 Ah with an arrangement of 55 in parallel and 55 in series. Each corresponds to a capacity of 10 Ah with a maximum OCV of 4.2V and a minimum of 2.5V.

2.4 Overall Connection

The overall system connection is presented in Figure 4, where the interaction and energy flows between the different components are shown. Here, the electrical cabinet is in charge of distributing the different flows to each equipment. The system is simulated for 4 years with a time step of 15 minutes, where for the 1st and 2nd years, the DHN and the balancing electricity market are not connected, and only the energy reservoirs are charging with heat. After this time, the system starts to operate at full capacity, i.e. all the components work simultaneously.
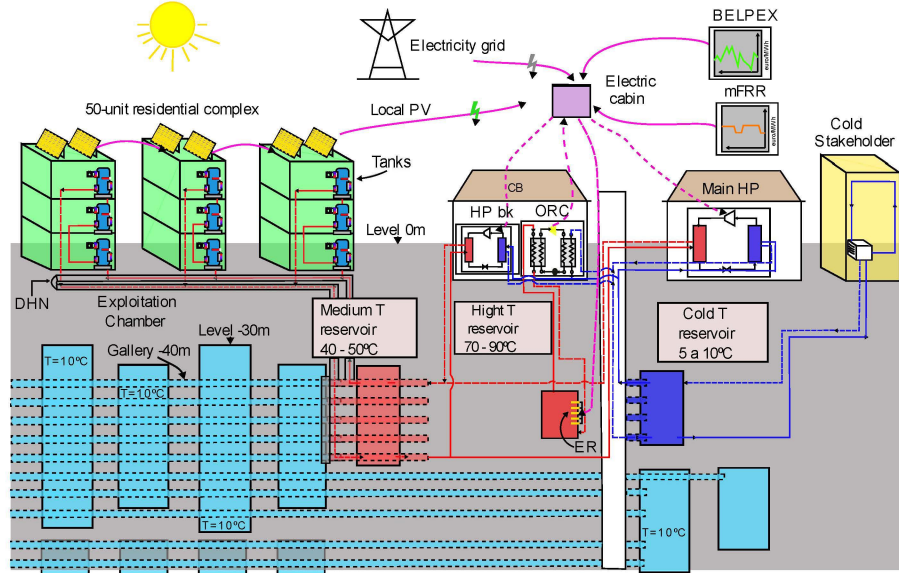

Figure 4: Overall connection of the assessed system, representing the whole connection and distribution.

The following assumptions are considered in the simulation. The system is allowed to operate in both electricity markets. Additionally, when the mFRR signal is activated, the ORC or ER operates under nominal capacity, there are no partial operations if the energy bids are lower than the capacity. Furthermore, given that the system contributes to increasing the resilience of the electricity grid and the share of RES, it is considered that ELIA will rank first in the order of merit, allowing it to operate in 100% of the cases of balancing activation, which can be supported by the system power capacities that do not generate a considerable effect in the energy bids. To reduce the simulation time, the most affected apartment by solar radiation is identified to replace the computation time of the 50 apartments. Subsequently, this effect is incorporated into the overall simulation by amplifying it 50 times for both the auxiliary equipment at the apartment level and the energy extracted from the DHN.

The global indicators assessed in this study include store efficiency presented in Equation 1. The global COP of the system is in Equation 2, excluding the HT components since it does not supply energy for heating purposes at the end-users. The ORC efficiency is presented in Equation 3, which is subsequently used to calculate the Round Trip Efficiency (RTE). Equation 4 outlines the revenue obtained from the electricity services provided by the CB, valid for both BELPEX and imbalance calculations.

$$\eta_{sto} = \frac{\int_{t_{in}}^{t_f} \dot{m}_{w,DHN} \cdot c_{p,w} \cdot \left(T_{w,su,DHN} - T_{w,ex,DHN}\right) dt}{\sum \int_{t_{in}}^{t_f} \dot{m}_{w,HP,j} \cdot c_{p,w} \cdot \left(T_{w,ex,HP,j} - T_{w,su,HP,j}\right) dt} \tag{1}$$

$$COP_{SUSTES} = \frac{\int_{t_{in}}^{t_f} \dot{Q}_{build}(t) + \dot{Q}_{DHW}(t) \, dt}{\int_{t_n}^{t_f} \sum \dot{W}_{aux}(t) + \sum \dot{W}_{cp,HP,j}(t) + \sum \dot{W}_{tk,app}(t) \, dt} \tag{2}$$

$$\eta_{ORC} = \int_{t_{in}}^{t_f} \frac{\dot{W}_{exp,ORC}(t) - \dot{W}_{pp,ORC}(t)}{\dot{Q}_{ev,ORC}(t)} dt \tag{3}$$

$$Revenues = \sum_{k=t_{in}+1}^{k=t_f} \frac{\int_{t_{k-1}}^{t_k} \dot{W}_{CB}(t) \, dt}{3.6 \cdot 10^9} \cdot Price_k(t) \tag{4}$$

3. RESULTS AND DISCUSSION

The simulation results are discussed in this section. The main idea of this system is to give a new purpose to abandoned mines, which are currently an unused space. In this paper the abandoned caverns are used to store energy, aiming to cover as much as possible of the heat demand of a 50-apartment housing complex, to generate a cold reservoir that can be used by any stakeholder close to the mine, and also to participate in balancing services of the electricity grid. To achieve this, during the first two years of operation, the energy is used to heat the water inside the reservoirs, as well as to heat the surrounding slate rocks. Figure 5a presents the cavern heat losses during the simulation for the LT, MT and HT reservoirs. It is possible to observe that in the 1st and 2nd years, the heat losses are crucial and indispensable for operation in further years, as part of this heat is recovered from the slates surrounding the reservoirs. Therefore, as presented, the heat losses decrease and the heat recovered increases over the years. In the case of the LT reservoir, the heat losses are mainly negative as the temperature is lower than the soil temperature. Figure 5b illustrates the temperature of the reservoirs, where in the case of the MT reservoir, the heat recoveries from the slates rocks occur in the periods of discharge of them.
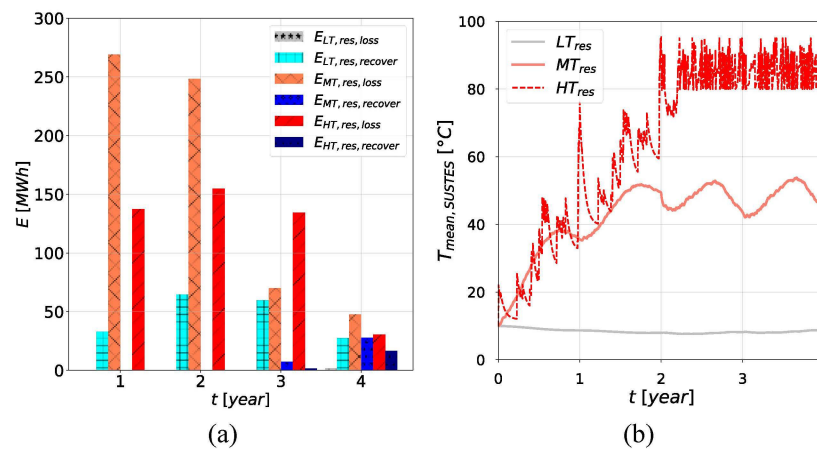

(a)   (b)

Figure 5: LT, MT and HT Underground reservoirs a) heat losses and b) average temperature during the simulation.

On the other hand, this temperature variation shows that the SUSTES (MT-reservoir) presents a seasonal behaviour, oscillating during the years of operation, being charged during the summer, and partially discharged during the winter. Resulting in recovery energy ($E_{i,res,recover}$) from the rocks. Moreover, it can be appreciated for the HT reservoir the rapid discharge time during the first two years, which is related to heat losses. During this period, the HT is charged by the bk HP and the ER, in parallel only when the price of the BELPEX is lower than 0 €/MWh. Subsequently, when the system starts operating, it is possible to appreciate the conservation of the temperature levels in the reservoir, reaching a maximum of 95°C and a minimum of 80°C, which represents the charging and discharging of the reservoir by the ORC and the electrical resistances (ER).

Figure 6 presents the energy produced by each HP during the 4 years of operation. In this case, the bk HP in the 1st and 2nd years follows the condition mentioned above, being able to generate 17 MWh during this period. The heat demand of the residential complex (SH + DHW) corresponds to a total of 569.2 MWh, with a value of 182.5 MWh for DHW. During the 1st and 2nd years, only the DHW demand is considered in the simulation and is covered by the tank in each apartment. In the 3rd year, when the system starts operating, it can be seen that part of the heat demand is covered by the DHN, almost 77.4% of the total demand, whereas the remaining is covered by the HPs and ER at the apartment tank. The energy produced by the PV installation is almost all self-consumed by the main HP, remaining only a small surplus which decreases over the years as the reservoir temperature increases and thus the energy consumption for heating water through the main HP increases, reaching an average PV self-consumption factor of 91.7%. The average COP of the system corresponds to 2.73, which compares the total heat supplied by all equipment contributing to the heating demand, and the total electrical energy required as input. The η_{sto} of the SUTES corresponds to 92.7%, which indicates that only 7.3% cannot be extracted from the storage tank, during 3rd and 4th year. Additionally, heat losses decrease considerably compared to the first years of operation, from 57% of the total energy given in the first year to 69% in the second year and then reach an average of 11% over the years of operation.
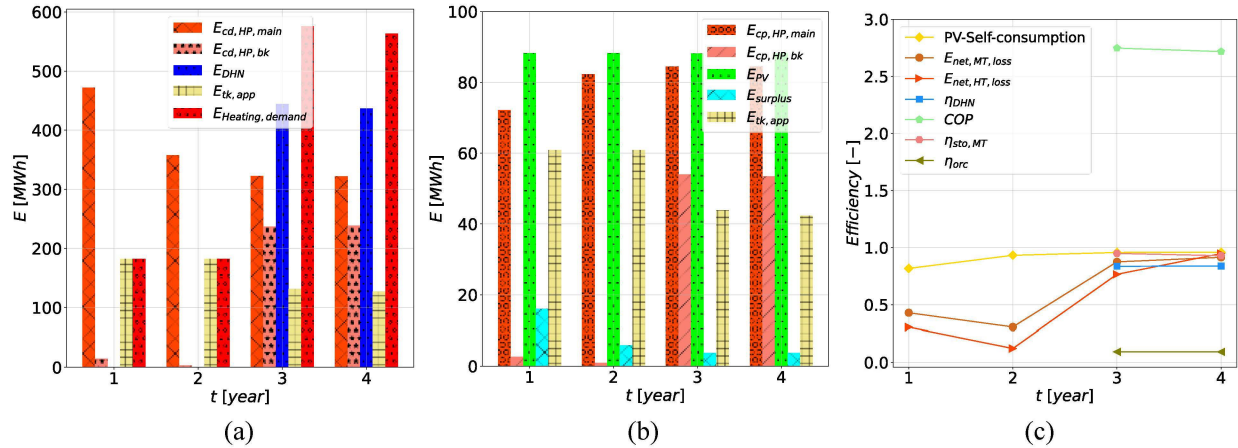
Figure 6: Annual performance for a) thermal energy, b) electrical energy, and c) overall performance coefficients.

The response of the system in the balancing or ancillary services of the grid is presented in Figure 7. Here, when the mFRR signal is downward, 800 kW of electrical resistance is used to reduce the excess electricity in the network. It is important to note that the main strategy is that the system is always available to operate in the balancing market, however, in the first two years the DAM market is used to consume electricity from the grid, using ER and the bk HP. Furthermore, the ERs have a higher monetary revenue due to the largest energy capacity. The ORC injects electricity into the grid when the DAM price is higher than 100 €/MWh, during the 3rd and 4th years. The main profits of the system are presented for the balancing grid market, in Figure 7. It is also appreciated that there is a gap between the revenues obtained from the DAM and mFRR. The market which generates the most gains in this system corresponds to the mFRR downward. The total revenue received from the CB system corresponds to a value of 41.6 thousand € the 3rd year and 44.2 thousand € in the 4th year. The ERs revenue corresponds to 86.4% and 83.7% of the total value, for the 3rd and 4th, respectively. The ORC efficiency corresponds to 9.2%, leading to a system RTE of 25.1%.
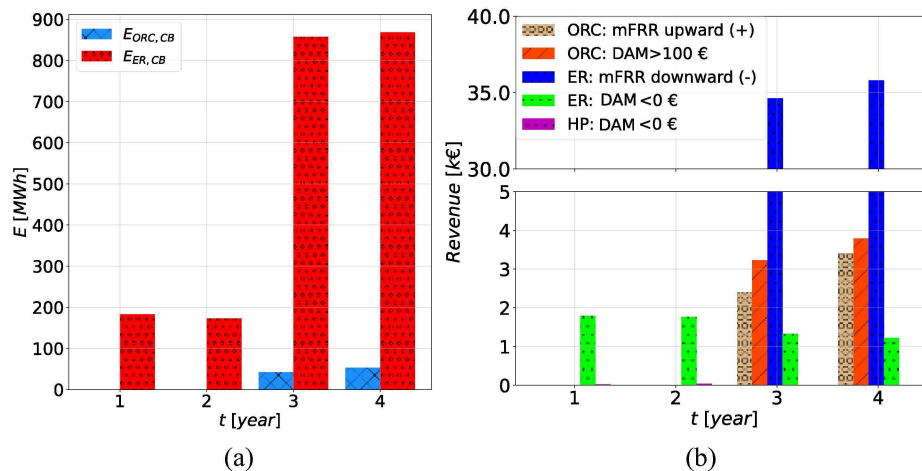

Figure 7: a) Energy produced by the ORC and electrical resistance with b) their respective revenues.

The system's performance in the electricity market is presented in Figure 8 for two days of operation. This graph shows that the highest revenues are attributed to the downstream mFRR (90.8 €), where the energy is higher than the ORC. Furthermore, for the ORC the higher revenues (86.4 €) are in the DAM market. The variations in the HT reservoir SOC (HT-SOC) represent the charge and discharge during the two days of operation, the SOC is considered 100% within 95°C and 0% within 80°C. Furthermore, the ORC can operate at nominal conditions as long as the HT reservoirs remain at 90°C (HT-SOC = 66.7%), producing 48 kWe.

There are still gaps in the system to increase revenues from electricity arbitrage. The selection of the optimal operating threshold of the system is a step that has not yet been addressed. The current value (100 €/MWh) has an operating time of 4200 hours while lowering it to 80 €/MWh increases the operating hours to 5330.
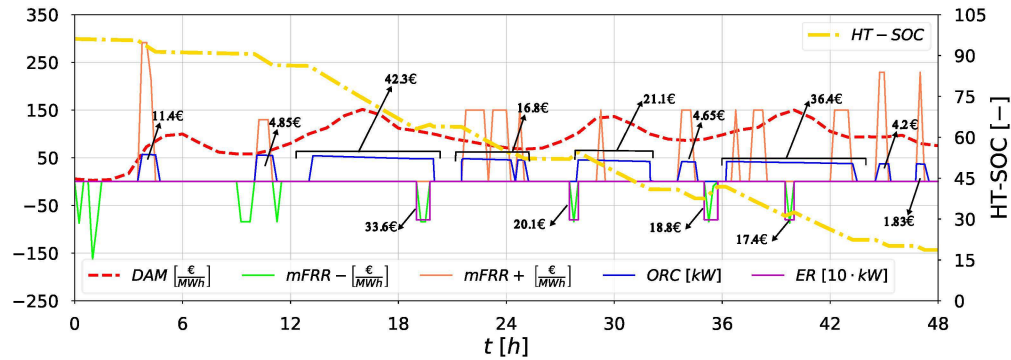
Figure 8: System operation during two days, electricity withdrawals and injections with their respective revenues.

4. CONCLUSIONS

The study presents insight into an innovative system in a real case in the southern of Belgium, given a new use for the abandoned mines. The system integrates a solar park for producing green energy to be stored in a SUSTES, with a PV self-consumption factor of 91.7%. This reservoir uses heat pumps for storing large production during summer to cover 77% of the total heating demand of 50 apartments (SH and DHW) throughout a DHN. The COP of the system reaches 2.73 for the whole year of operation. Additionally, this system incorporates an ORC where the start-up and shutdown are incorporated by a second-order transfer function based on experimental data. The system is coupled to ERs, thus providing a balance to the electrical services, specifically in the tertiary service mFRR, besides the system participating in the DAM. The system can generate a revenue of 7.2 thousand € in ORC mode over 1 year of operation, where the higher revenues are related to DAM price, and 37 thousand € for the downward control of the mFRR, taking an average of 862 MWh per year. These results are taken based on the 2023 price of the electricity market assuming that the ELIA will give us the maximum prioritization in the merit order, and without considering any fee from the Belgian government specifically (ORES TSO). The study works as a price stalker, which gives an insight into the maximum revenues that can be obtained in the electricity market from a multi-energy system able to supply heat, power and cooling to the stakeholders. On the other hand, an increase in revenue has not been addressed yet, nevertheless is clear that there is a gap in the threshold selected for the DAM market, as well as between the operation preference of the system in both markets. This system could also participate in the aFRR market, as the dynamic response of the system is less than 7.5 min, which would increase the revenues that could be generated by balancing the grid.

NOMENCLATURE

c_p	Specific Heat	(J/kg-K)	cd	Condenser	
CB	Carnot Battery	(−)	cp	Compressor	
COP	Coefficient of Performance	(−)	demand	Demand	
DHN	District Heating Network	(−)	ev	Evaporator	
DWH	Domestic Hot Water	(−)	ex	Exhaust	
E	Energy	(MWh)	exp	Expander	
ER	Electrical resistances	(−)	f	Final	
HP	Heat Pump	(−)	heating	Heating	
$\dot{m}$	Mass Flow Rate	(kg/s)	HT	High Temperature	
N	Rotation speed	(Hz, rpm)	in	Initial	
NRV	Net Regulation Volume	(MW)	loss	Losses	
OCV	Open Circuit Voltage	(−)	LT	Low Temperature	
ORC	Organic Rankine Cycle	(−)	main	main HP	
PV	Photovoltaics panels	(−)	MT	Medium Temperature	
$\dot{Q}$	Heat Flow Rate	(kW)	Net	Net	
t	Time	(h, year)	pp	pinch point, pump	
T	Temperature	(°C)	recover	Recovered	
$\dot{W}$	Power	(kW)	res	Reservoir	
Greek letters			s	Isentropic	
η	Efficiency	(−)	sc	Subcooling	

ε	Efficacy	(–)	sh	Superheating
Δ	Difference	(–)	sto	Storage
λ	Thermal conductivity	(W/mK)	su	Supply
ρ	Density	(kg/m^3)	surplus	Surplus
Subscript			tk	Tank
app	Apartment		v	Volumetric
aux	Auxiliary		w	Water
build	Buildings		wf	Working fluid
bk	back-up HP			

REFERENCES

Cabeza, L. F. , Q. Bai, P. Bertoldi, J.M. Kihila, A.F.P. Lucena, É. Mata, S. Mirasgedis, A. Novikova, & Y. Saheb. (2022). Buildings. In IPCC, 2022: Climate Change 2022: Mitigation of Climate Change. In *Contribution of Working Group III to the Sixth Assessment Report of the Intergovernmental Panel on Climate Change* (pp. 953–1048). Cambridge University Press. https://doi.org/10.1017/9781009157926.011

Crawley, D. B., Lawrie, L. K., Winkelmann, F. C., Buhl, W. F., Huang, Y. J., Pedersen, C. O., Strand, R. K., Liesen, R. J., Fisher, D. E., Witte, M. J., & Glazer, J. (2001). EnergyPlus: creating a new-generation building energy simulation program. *Energy and Buildings*, *33*(4), 319–331. https://doi.org/10.1016/S0378-7788(00)00114-6

Desideri, A. (2016). *Dynamic modeling of organic Rankine cycle power systems* [University of Liège]. https://orbi.uliege.be/handle/2268/204267

Desideri, A., Hernandez, A., Gusev, S., van den Broek, M., Lemort, V., & Quoilin, S. (2016). Steady-state and dynamic validation of a small-scale waste heat recovery system using the ThermoCycle Modelica library. *Energy*, *115*, 684–696. https://doi.org/10.1016/j.energy.2016.09.004

Duffie, J. A., & Beckman, W. A. (1991). *Solar Engineering of Thermal Processes* (Jhon Wiley & Sons Inc., Ed.; 2nd ed.).

Dumont, O., Frate, G. F., Pillai, A., Lecompte, S., De paepe, M., & Lemort, V. (2020). Carnot battery technology: A state-of-the-art review. *Journal of Energy Storage*, *32*. https://doi.org/10.1016/j.est.2020.101756

Grabenweger, P., Lalic, B., Trnka, M., Balek, J., Murer, E., Krammer, C., Možný, M., Gobin, A., Şaylan, L., & Eitzinger, J. (2021). Simulation of daily mean soil temperatures for agricultural land use considering limited input data. *Atmosphere*, *12*(4). https://doi.org/10.3390/atmos12040441

Jin, H. (2002). *Parameter estimation based models of water source heat pumps* [Oklahoma State University]. https://hdl.handle.net/11244/46835

Jorissen, F., Reynders, G., Baetens, R., Picard, D., Saelens, D., & Helsen, L. (2018). Implementation and verification of the ideas building energy simulation library. *Journal of Building Performance Simulation*, *11*(6), 669–688. https://doi.org/10.1080/19401493.2018.1428361

Ljung, L. (1999). System identification: theory for the user. *PTR Prentice Hall, Upper Saddle River, NJ*, *28*, 540.

Luo, X., Wang, J., Dooner, M., & Clarke, J. (2015). Overview of current development in electrical energy storage technologies and the application potential in power system operation. *Applied Energy*, *137*, 511–536. https://doi.org/10.1016/j.apenergy.2014.09.081

Olympios, A. V., McTigue, J. D., Farres-Antunez, P., Tafone, A., Romagnoli, A., Li, Y., Ding, Y., Steinmann, W. D., Wang, L., Chen, H., & Markides, C. N. (2020). Progress and prospects of thermo-mechanical energy storage-a critical review. In *Progress in Energy* (Vol. 3, Issue 2). Institute of Physics. https://doi.org/10.1088/2516-1083/abdbba

Poletto, C., Dumont, O., De Pascale, A., Lemort, V., Ottaviano, S., & Thomé, O. (2024). Control strategy and performance of a small-size thermally integrated Carnot battery based on a Rankine cycle and combined with district heating. *Energy Conversion and Management*, *302*. https://doi.org/10.1016/j.enconman.2024.118111

Wetter, M., & Van Treeck, C. (2017). *New Generation Computational Tools for Building & Community Energy Systems Annex 60*. www.iea-ebc.org

ACKNOWLEDGEMENT